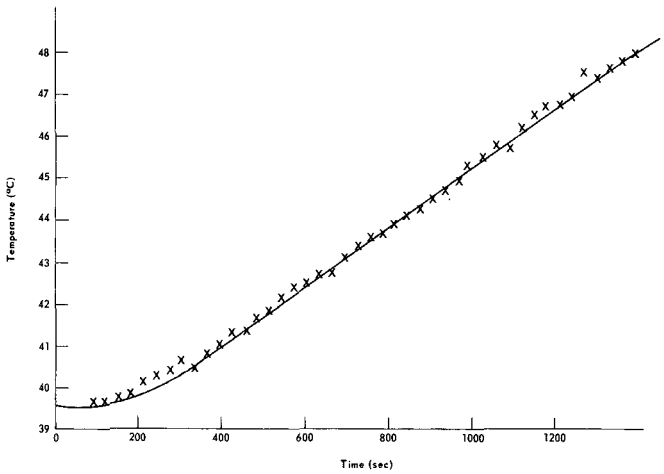

Fig. 6. Temperature data and least square fit.

Y_0 = value of Y at original steady state
Y_f = value of Y at final steady state
Z_i = data point
τ_1 = calculated major time constant
τ_1^0 = actual major time constant
τ_2 = calculated minor time constant
τ_2^0 = actual minor time constant

LITERATURE CITED

Bacher, S., A. Kaufman, "Computer-Controlled Batch Chemical Reactions," *Ind. Eng. Chem.*, **62**, 53 (1970).

Gaspar, T. G., et al., "New Process Language Uses English Terms," *Contr. Eng.*, 118 (1968).

Koppel, L. B., and P. R. Latour, "Time Optimal Control of Second-Order Overdamped Systems with Transportation Lag," *Ind. Eng. Chem. Fundamentals*, **4**, 463 (1965).

Lapidus, L., Digital Computation for Chemical Engineers, p. 21-25, McGraw-Hill, New York (1962).

Latour, P. R., L. B. Koppel, and D. R. Coughanowr, "Time-Optimal Control of Chemical Processes for Set-Point Changes," *Ind. Eng. Chem. Process Design Develop.*, **6**, 452 (1967).

Law, V. J., and R. V. Bailey, "A Method for the Determination of Approximate System Transfer Functions," *Chem. Eng. Sci.*, **18**, 189 (1963).

Mellichamp, D. A., "Model Predictive Time-Optimal Control of Second-Order Processes," *Ind. Eng. Chem. Process Design Develop.*, **9**, 494 (1970).

Miller, J. A., et al., "Use of Search Techniques to Determine Optimal Switching Times," paper presented at AIChE Meeting, New Orleans (1969).

Pontryagin, L. S., et al., The Mathematical Theory of Optimal Processes, Chap. 3, Wiley, New York (1962).

Seifert, W. W., and C. W. Steeg, Control System Engineering, p. 253-255, McGraw-Hill, New York (1960).

Shinskey, F. G., and J. L. Weinstein, "A Dual-Mode Control System For a Batch Exothermic Reactor," paper presented at 20th Annual ISA Conf., Los Angeles, Calif. (1965).

Steadman, J. B., and L. B. Koppel, "Bang-Bang Control is Faster," *Hydrocarbon Processing*, **51**, No. 7, 101 (1972).

Manuscript received March 13, 1972; revision received June 20, 1972; paper accepted June 21, 1972.

Fixed-Bed Desorption Behavior of Gases With Non-Linear Equilibria:

Part I. Dilute, One Component, Isothermal Systems

Generalized depletion curves for desorption (and breakthrough curves for adsorption) were calculated for a system characterized by the Langmuir-type equilibria and controlled by a film type rate model. The depletion points generally appear sooner than the corresponding breakthrough points, and the desorption profiles are significantly broader than the corresponding adsorption curves. These phenomena may be best explained in terms of the prevailing driving forces. The effects of adsorbate properties and operating variables (inlet composition and flow rate) were established and experimentally substantiated.

IMRE ZWIEBEL
ROGER L. GARIEPY
and
JAY J. SCHNITZER

Worcester Polytechnic Institute
Worcester, Massachusetts 01609

SCOPE

If both the adsorption and desorption operations in fixed beds could be described as first-order linear processes, the desorption profiles, or depletion curves, would be mirror images of the adsorption breakthrough curves. However, experiments have shown that even when the desorption step was carried out as an identical opposite of the adsorption, that is, same flow rate, same temperature, etc., a longer time was needed on desorption to return the bed to its initial starting condition than was allowed for the previous adsorption step.

To accommodate these differences, processes have been designed with pressure swing cycling, with elevated temperature regeneration, or even with chemical displacement

desorption. Often, these additional processing requirements involve the inclusion of a costly third bed in the design; as one bed is being used for adsorption, the other two are on the regeneration cycle to provide the extra operating time for purging or to allow the return of temperature or pressure to the appropriate adsorption levels.

The deviations from the mirror-image relationship between adsorption and desorption profiles have been attributed to observed nonlinearities, especially in the adsorption isotherm. Heretofore, only the adsorption portion of the operation has received much attention in the literature, and simulation even of this portion required the use of a complex rate model to facilitate the mathematical derivations. The objective of this paper is to present depletion data for fixed bed regeneration and to account for the effects of isotherm nonlinearities.

CONCLUSIONS AND SIGNIFICANCE

Using the film model to describe the mass transfer mechanism and the Langmuir-type isotherm equation to account for the nonlinearities in the equilibrium data, both desorption and adsorption profiles were calculated. The two parameters, which can be used to describe the isotherm nonlinearity (the equilibrium constant K and the gas inlet composition c_0), can also be used to characterize the desorption depletion curves and the adsorption breakthrough curves. With increasing isotherm curvature, that is, higher values of K, both the breakthrough points and depletion points are delayed, and the concentration-time profiles are broadened. With increasing inlet concentrations, the opposite effects are obtained, that is, breakthrough and depletion times are reduced and the concentration profiles are sharpened. These phenomena may be explained in terms of the prevailing adsorption or desorption rates. At the beginning of the run, the desorption rates are generally higher; hence, the depletion times will be shorter than the breakthrough times. As the processes progress there is a crossover in the rate curves, and the adsorption rates reach significantly higher peak values. Ultimately the desorption rates recede to zero much more slowly than do the adsorption rates, resulting in the prolonged tail in the depletion curves.

Thus, it is readily seen that extra effort must be expended during the adsorbent regeneration portion of a separation process. The results presented in this paper may be used to carry out design calculations which take into account the dissimilarities between adsorption and desorption. While these data are based on a simple mechanistic model used to describe the physical phenomena, that is, the film model, they provide a first step in improved design criteria. In addition, these results represent the first publication of generalized depletion data for systems described by nonlinear isotherms.

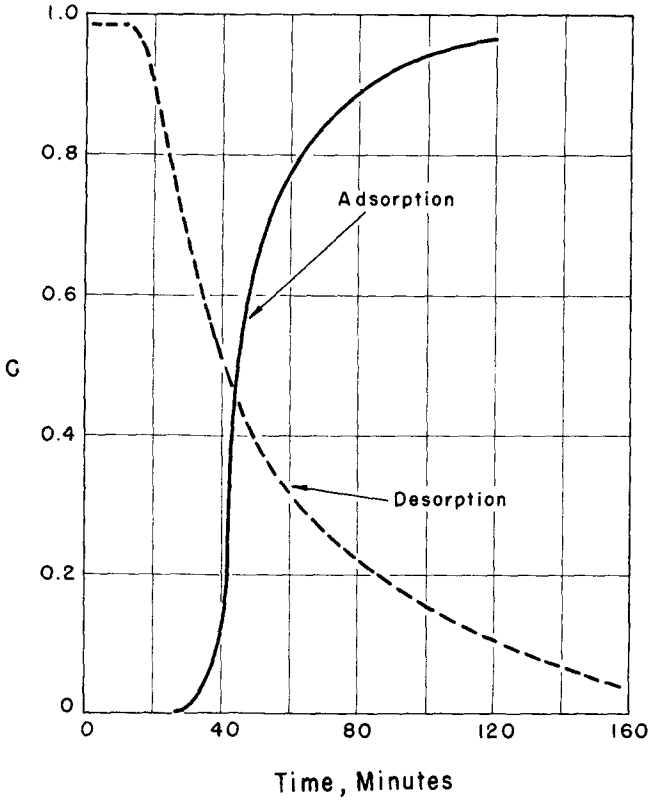

Fig. 1. Experimental adsorption breakthrough curve and desorption depletion curve; C_2H_6 on charcoal, $L = 180$ cm.; $F(N_2) = 15{,}000$ s. cc./min, $c_0 = 1\%$ C_2H_6 in N_2 carrier.

The widespread application of separation processes based on adsorption/desorption and the relatively high cost and sensitivity of the recently developed specialty adsorbents dictate that during the design of facilities closer attention be paid to the regeneration step. Reinforcing this need are observations made in the laboratory, like the data presented in Figure 1, or in commercial applications, that is, the heatless adsorption process. In this latter example a penalty is paid by the use of increased purge-gas flow rates during desorption in comparison with the gas loads carried during adsorption. To account for this nonsymmetrical behavior, it has been suggested that the cyclic processes be designed by using the generalized data previously published in the literature for linear systems, that is, Hiester and Vermeulen (1952) or Eteson and Zwiebel (1969), with different empirically derived coefficients for adsorption and desorption (Fukunaga et al., 1968).

Kondis and Dranoff (1971) investigated the internal diffusive transport mechanism in molecular sieves, and they attributed the difference between adsorption and desorption primarily to isotherm nonlinearity, and stipulated that these effects were more significant than the prevailing temperature effects. Similarly, Timofeev (1958), Kurochkina and Romankov (1960), and Nassonov (1961) reported equilibrium effects on the desorption versus adsorption behavior of gases and vapors. This strongly suggests that the linear analyses mentioned above would not be expected to provide satisfactory designs. Hiester and Vermeulen (1952) treated a special adsorption case with nonlinear equilibrium when they applied the reaction kinetics model developed by Thomas (1944). However, up to now only empirical treatments of desorption have

been published (Hiester et al., 1963). In this paper calculated depletion data for fixed bed regeneration are presented with both linear and favorable nonlinear isotherms, and they are contrasted with the breakthrough behavior.

EXPERIMENT

In our own experiments studying the dynamic behavior of fixed bed adsorption columns (Gariepy, 1972; Zwiebel and Schnitzer, 1971), nonsymmetrical breakthrough and depletion curves were observed even when attempts were made to establish identical operating conditions for the two experiments (that is, same temperature and flow rate with dilute adsorbate levels). For example, Figure 1 illustrates the corresponding effluent concentration profiles from a 180 cm. long activated charcoal column adsorbing C_2H_6 from an N_2 stream at a carrier flow rate of 15,000 s. cm³/min. The inlet composition during adsorption was 1% C_2H_6 by volume and was charged as a step input into a freshly activated, nitrogen purged column; desorption was also initiated as a step-function change in concentration from the 1% C_2H_6 feed into the saturated column to a C_2H_6-free nitrogen stream. The nitrogen flow rates were maintained constant at all times; whenever necessary the small (150 s. cm³/min.) C_2H_6 stream was added. The C_2H_6 composition was continuously measured by a flame ionization detector and recorded. The temperature of the system was monitored and no significant deviation was observed from the ambient inlet conditions. Thus, it may well be approximated that the adsorption and desorption steps were carried out under nearly identical conditions; nevertheless, significant differences were obtained between the breakthrough and depletion curves.

Similar results were observed at a variety of operating conditions. The differences between the adsorption and desorption results (that is, breakthrough times versus depletion times, width of adsorption zone versus depletion zone, slope of breakthrough curve versus slope of depletion curve at the 50% point of the composition profile, etc.) were always proportional to the variables which emphasized the nonlinearity of the isotherm. For example, increasing differences between adsorption and desorption were measured in the same order as the relative equilibrium nonlinearities of the various adsorbates were increasing ($CO_2 < C_2H_4 < C_2H_6$; Figure 2). In contrast, however, varying operating conditions such as gas inlet flow rate, which do not directly influence the equilibrium, did not exert such proportional effects upon these differences.

ANALYSIS

To analyze the dilute, one component, isothermal adsorption/desorption phenomena in a fixed bed, the usual (Vermeulen, 1958; Eteson and Zwiebel, 1969) adsorbate mass balance was written on the gas phase

$$\frac{\partial C}{\partial v} + \frac{1}{A}\frac{\partial C}{\partial u} + \frac{\partial W}{\partial u} = 0 \qquad (1)$$

with a film type rate expression assumed to describe the mass transfer phenomenon

$$\frac{\partial W}{\partial u} = C - C^* \qquad (2)$$

where the dependent variables C and W have been normalized with respect to c_0 and w_s (w_s is the equilibrium loading which corresponds to the inlet gas composition c_0), and the independent variables were defined as follows:

$$\text{dimensionless distance parameter } v = \frac{kx}{V} \qquad (3a)$$

$$\text{dimensionless time parameter } u = \frac{kc_0}{\rho_B w_s} t \qquad (3b)$$

In writing Equations (1) and (2) a dilute feed composition of the adsorbate was assumed so that constant flow rates and isothermal operations could be simulated. Also, a linear first-order mass transfer rate was stipulated (with no internal transport), and the effects of axial dispersion as well as all radial profiles were neglected. Thus, the resulting simplified model is limited to handling only select systems. The more comprehensive problem, which includes nonisothermal behavior and competitive multicomponent sorption, will be treated in subsequent papers.

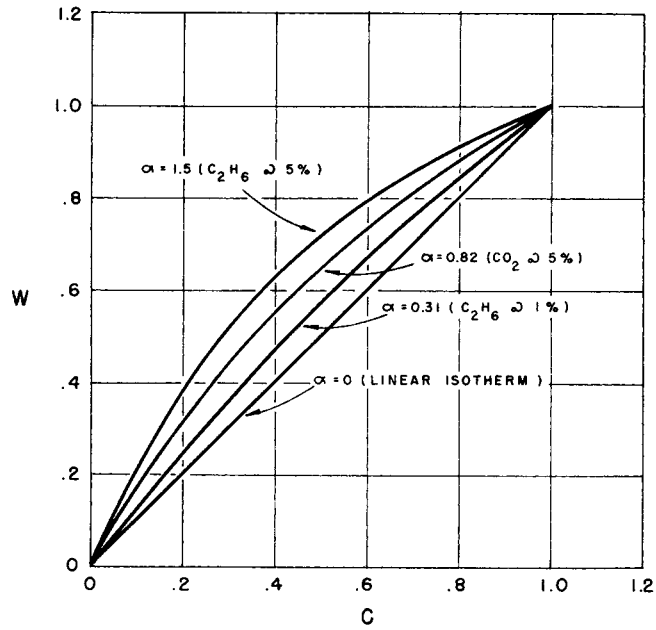

Fig. 2. Typical Langmuir-type isotherms illustrating component and gas composition effects on the degree of curvature.

The variable C^* is the normalized representation of the gas phase composition in equilibrium with the variable surface loading, that is, $C^* = f(W)$. In the early analyses linear isotherms

$$C^* = W \qquad (4a)$$

were written to enable solution of the equations. The assumption was deemed feasible since the feed stream during the adsorption was dilute. However, recent investigations with specialized high capacity adsorbents prompt the use of nonlinear equilibrium expressions. The Langmuir-type expression is preferred for computational reasons and because it is readily adaptable to interactive multicomponent systems (Gariepy and Zwiebel, 1971). Most of the time the expression is used as an empirical fit to the measured equilibrium data and does not imply adherence to the monolayer theory. Within the context of the present analysis, the nonlinear alternate to Equation (4a) may be written as follows:

$$C^* = \frac{W}{(\alpha + 1) - \alpha W} \qquad (4b)$$

where $\alpha = Kc_0$, and K is the Langmuir-type coefficient.

The boundary conditions for the desorption problem, with a step function elimination of the adsorbate from the feed, can be written as

$$C(v = 0, u) = 0.0 \qquad (5a)$$

$$C(v, u = 0) = F_2(v) \qquad (5b)$$

$$W(v, u = 0) = G_2(v) \qquad (5c)$$

The most commonly stipulated initial conditions are beds saturated with the feed gas used in the previous adsorption step, so that $F_2(v) = 1.0$ and $G_2(v) = 1.0$. Under these

conditions it is immaterial whether the desorption is in the same direction or in the opposite direction as was the previous adsorption step. If, however, the initial distributions $F_2(v)$ and $G_2(v)$ are not constants, the directions of the desorption will create mathematical complications which render the analysis complicated.

Experience has shown (Lapidus, 1962; Eteson and Zwiebel, 1969) that the Equations (1) and (2) require excessive computation times when finite difference schemes are used to set up the problem for digital computer solution. Therefore, the method of characteristics, as outlined by Acrivos (1956), was employed to transform the partial differential equations into ordinary differential equations, enabling relatively rapid solutions to be obtained along the straight line characteristics v = constant and $u = v +$ constant. The results obtained are given as generalized plots, separate plots for each of the values of α, the equilibrium parameter. Each series of plots presented below required about 6 minutes computer time for the adsorption case and about 10 minutes for the desorption case. Approximately half the CPU time was consumed by the execution of printout instructions. The RCA Spectra 70-46 computer was used in a batch mode operation.

The companion adsorption problem using Equations (1), (2), and (4b), along with the appropriate boundary conditions describing a step input of adsorbate into an initially empty column

$$C(v = 0, u) = 1.0 \tag{6a}$$

$$C(v, u = 0) = F_1(v) = 0 \tag{6b}$$

$$W(v, u = 0) = G_1(v) = 0 \tag{6c}$$

was also solved and the results were compared with the Thomas predictions presented by Hiester et al., (1963). Figure 11a illustrates the comparison between two breakthrough profiles ($\alpha = 1$ and $\alpha = 2$) of the present work using the film model and the Thomas solutions based upon the reaction kinetics model. The curves obtained by the two models intersect at two points, resulting in very good agreement near the saturation levels ($C > 0.9$) and in the vicinity of $C \approx 0.1$. In the intermediate region, $0.1 < C < 0.9$, the agreement between the two solutions is qualitatively satisfactory. However, at very low effluent concentrations, near breakthrough, significant differences were obtained. This observation points to serious differences (25% in the value of the breakthrough time at $C = 0.01$) between the models since in many design problems the breakthrough point is the parameter of greatest concern.

A more striking illustration of the differences between the models is shown in the depletion profiles on Figure 11b. Following the recommended procedures (Hiester et al., 1963) to calculate the desorption curves corresponding to the reaction kinetics model, large discrepancies were obtained between the results of the two models. This points to the importance of ascertaining the proper controlling mechanism. Experimental evidence indicates that the reaction kinetics model is most useful in ion-exchange design, while the film model prevails in most gas-solid adsorption systems, especially when nonporous adsorbents are used.

RESULTS AND DISCUSSION

The generalized plots of gas phase composition profiles presented in Figures 3 through 7 as a function of the dimensionless parameters may be used for the design of operating equipment. Due to the combination of coefficients into the dimensionless groupings which include some of the pertinent constants, the above figures do not clearly show the effects of changes in operating variables. Hence, representative data were extracted from these plots and are presented as separate figures to illustrate the significant effects of the nonlinear isotherms.

The systems described by the Langmuir-type isotherms require a second constant to characterize the departure from linearity, as contrasted with the linear case where a single equilibrium coefficient suffices. This is usually accomplished by using the coefficient K and the so-called "monolayer capacity" W_m (Young and Crowell, 1962):

$$w = \frac{W_m K c}{1 + Kc} \tag{7}$$

The latter is algebraically cancelled as the variables are normalized with respect to the inlet gas composition c_0 and its equivalent equilibrium loading w_∞. As a result of the normalization, c_0 will appear as the second parameter in the equilibrium equation:

$$\frac{w}{w_\infty} = \frac{(1 + Kc_0) \cdot (c/c_0)}{1 + (Kc_0) \cdot (c/c_0)} \tag{8}$$

The co-appearance of K and c_0 in the normalized expression and their subsequent combination into a single equilibrium parameter α [α is related to the r used by Vermeulen (1958), Equation (4b)] indicates that they will have parallel effects upon the driving force.

This influence of K and c_0 on the driving force portion of the rate expression can be seen in Figure 8, where calculated values of the difference $|C - C^*|$ are plotted as a function of time at a fixed point $v = 10$ from the inlet to the column.

During desorption an increase in α decreases the peak heights and shifts them to lower time values, while during adsorption the opposite occurs—the peak heights increase

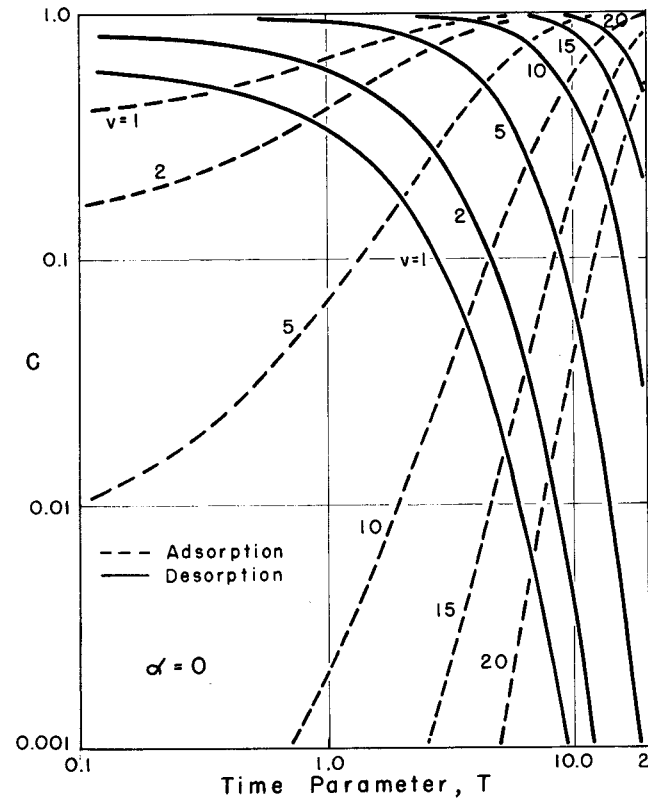

Fig. 3. Generalized breakthrough and depletion curves, C vs. T at $\alpha = 0.0$ (linear isotherm).

and are shifted to higher times as α increases.

This phenomenon explains the differences in behavior between adsorption and desorption. In the linear case ($\alpha = 0$), the driving force curves are identical for adsorbent loading and for regeneration steps, hence the mirror image breakthrough and depletion curves. But as the isotherms depart from linearity ($\alpha > 0$) significant differences can be observed (Figure 8):

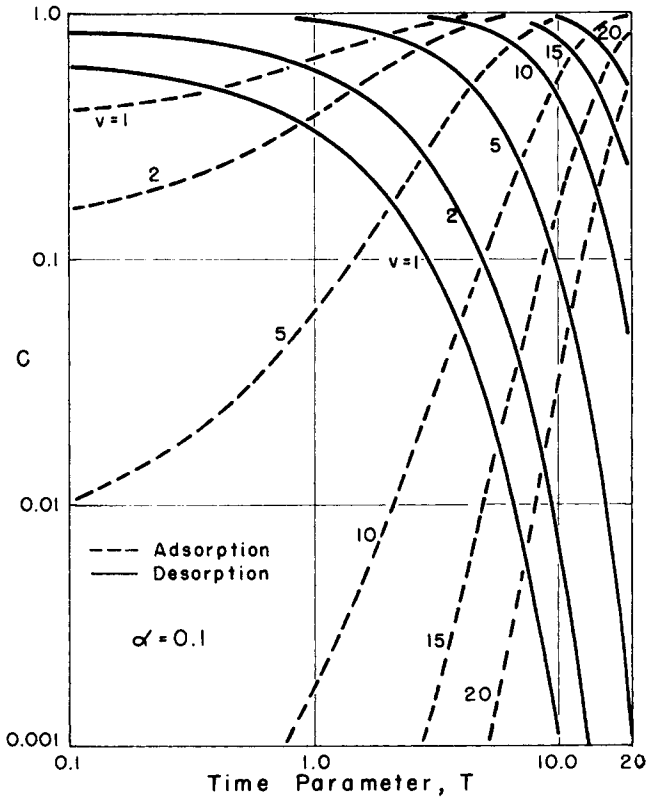

Fig. 4. Generalized breakthrough and depletion curves, C vs. T at $\alpha = 0.1$.

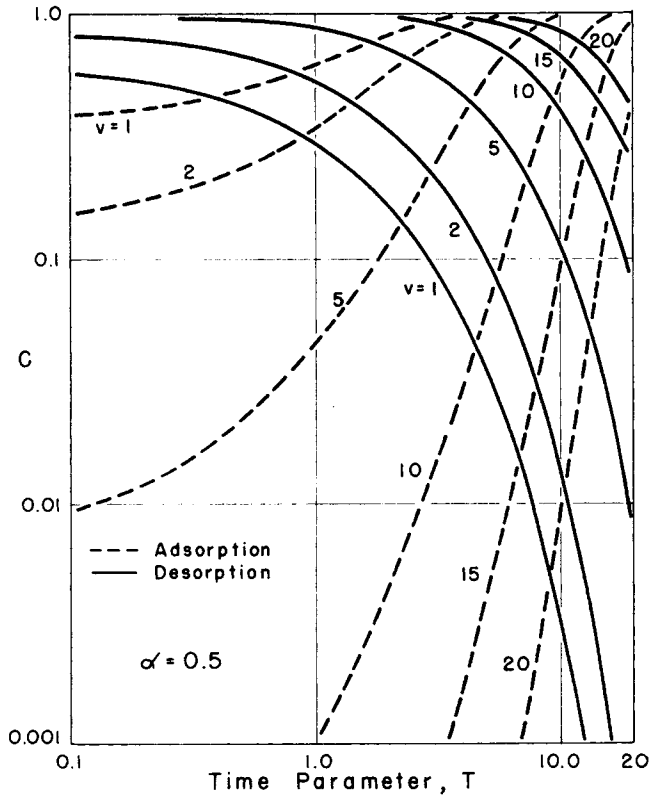

Fig. 5. Generalized breakthrough and depletion curves, C vs. T at $\alpha = 0.5$.

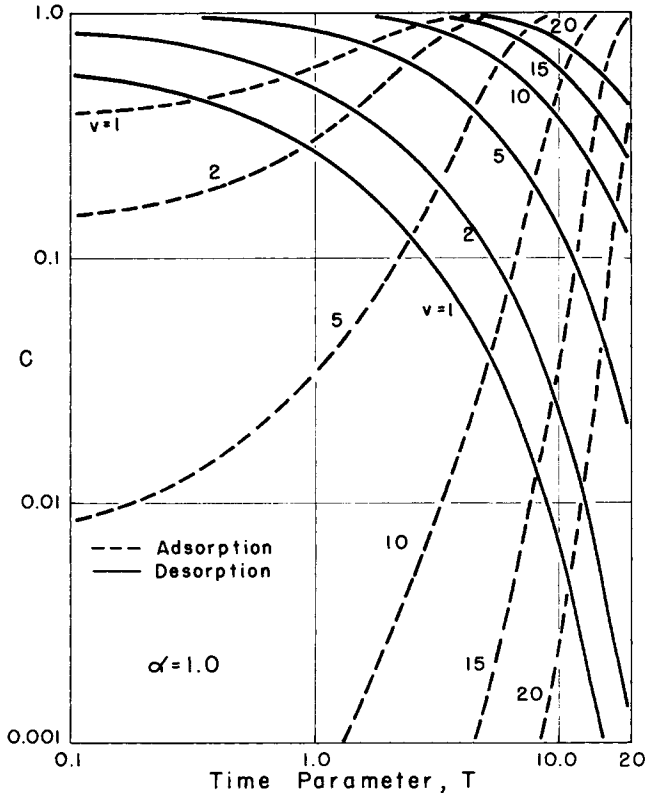

Fig. 6. Generalized breakthrough and depletion curves, C vs. T at $\alpha = 1.0$.

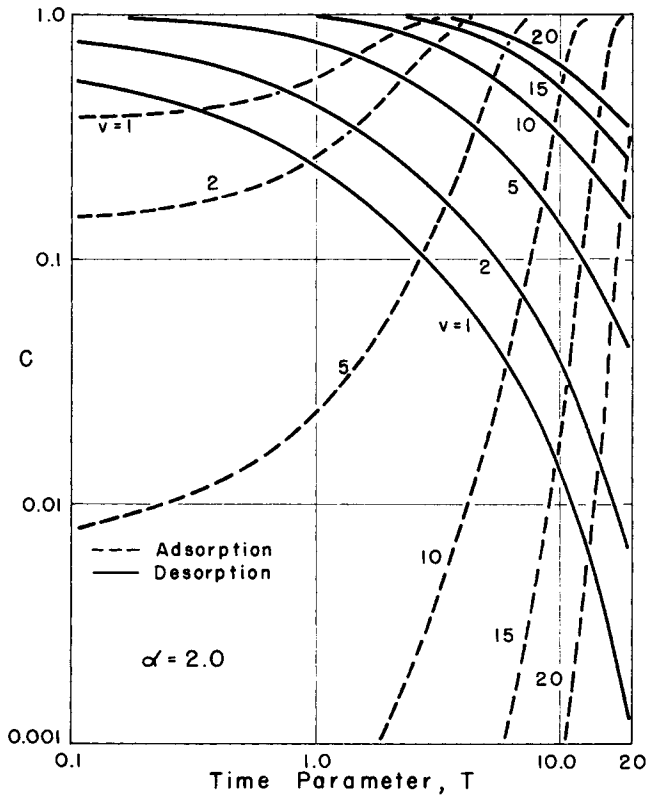

Fig. 7. Generalized breakthrough and depletion curves, C vs. T at $\alpha = 2.0$.

1. Initially the magnitudes of the desorption driving forces are larger, which means that desorption rates will be higher, and therefore the depletion points will appear sooner than the breakthrough points (see Figure 1). This concurs with the observations reported by Chi and Lee (1969).

2. As time proceeds the adsorption rates reach considerably higher values than do the desorption rates, which causes the sharper breakthrough profiles.

3. The peak values of the desorption driving forces are reached sooner than those of adsorption, thus the maximum slope of the depletion curves precedes the steepest portion of the corresponding breakthrough curves.

4. The desorption rates recede more slowly than do the adsorption rates, resulting in the extended tail of the depletion profiles.

Qualitatively these effects are illustrated in Figure 9 where along the isotherm typical operating curves are also drawn, and the horizontal lines at any point represent the driving forces. As a rule, in the desorption case these line segments are shorter, and they approach zero asymptoti-

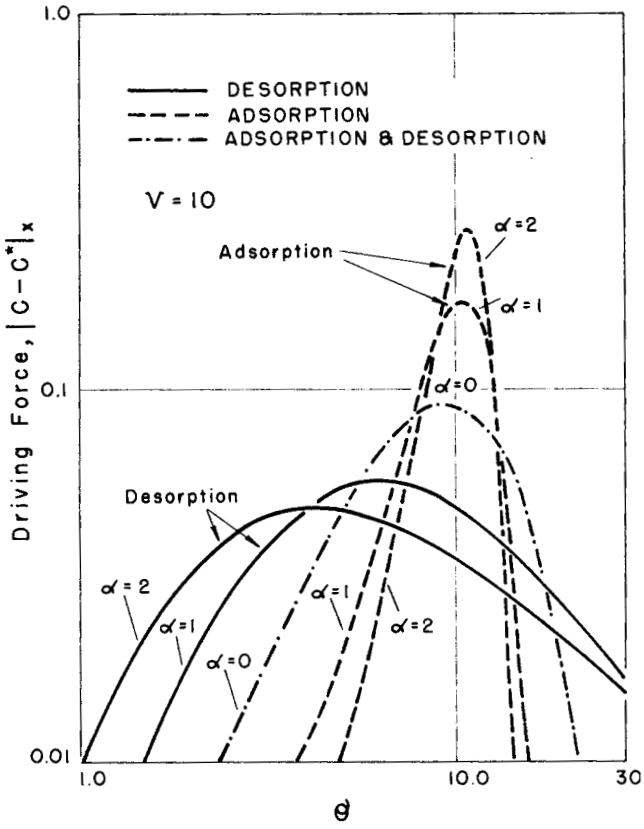

Fig. 8. Calculated adsorption and desorption driving forces as a function of time at fixed point $v = 10$.

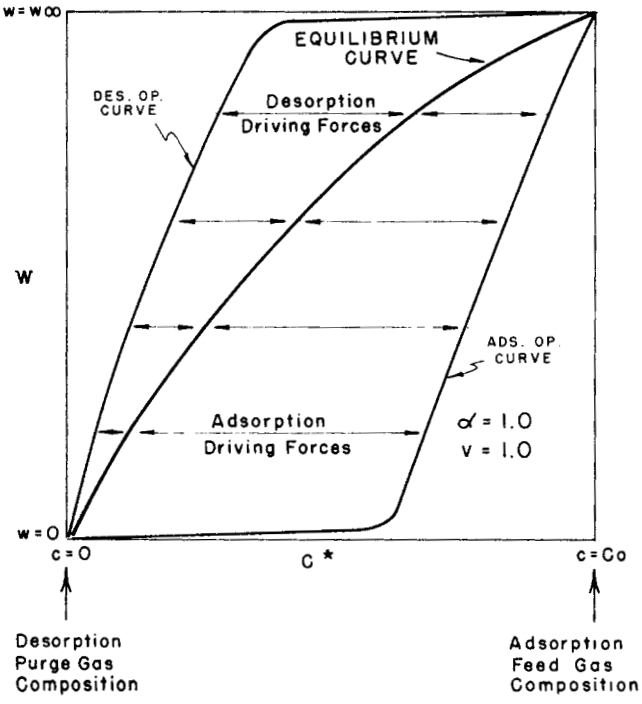

Fig. 9. Schematic diagram illustrating the magnitude of the driving forces during adsorption and desorption.

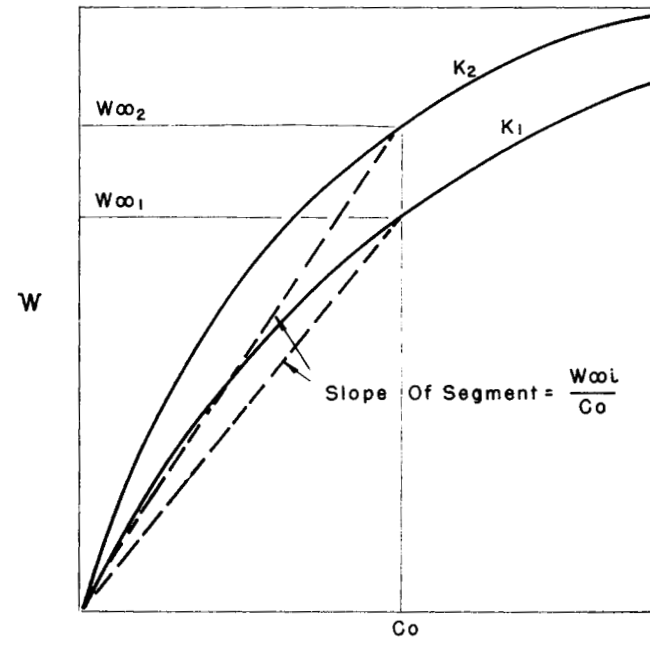

Fig. 10a. Schematic illustrating the effect of isotherm nonlinearity on the ratio w_∞/c_0, at $c_0 =$ constant.

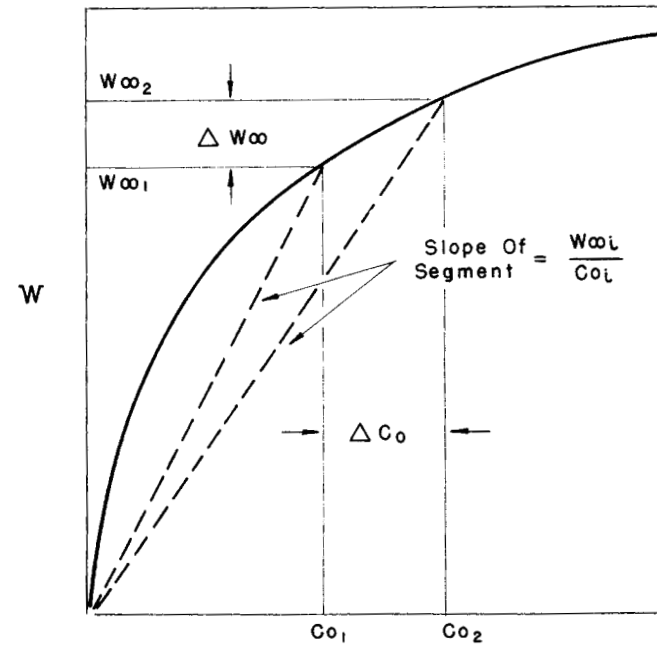

Fig. 10b. Schematic illustrating the effect of inlet composition on the ratio w_∞/c_0, at $K =$ constant.

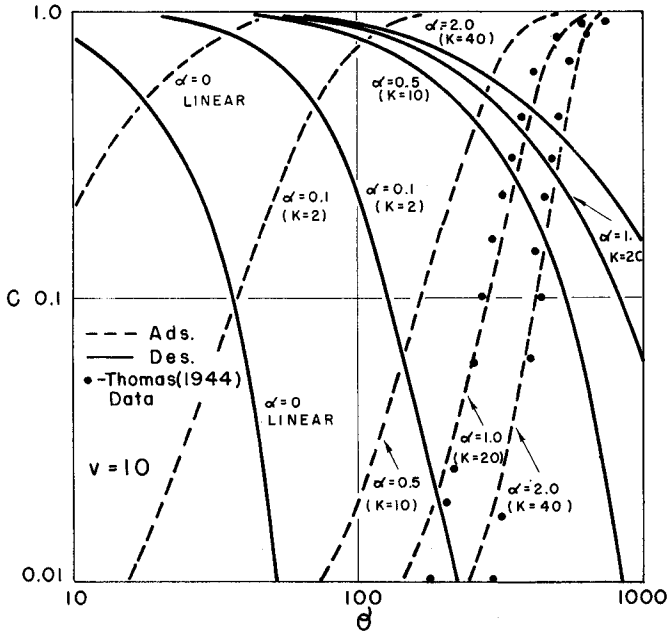

Fig. 11a. Calculated breakthrough and depletion curves at various values of the equilibrium constant K; c_0 = constant = 0.05; $\alpha = 0$ linear isotherm, for $\alpha > 0$ $K = \alpha/c_0$.

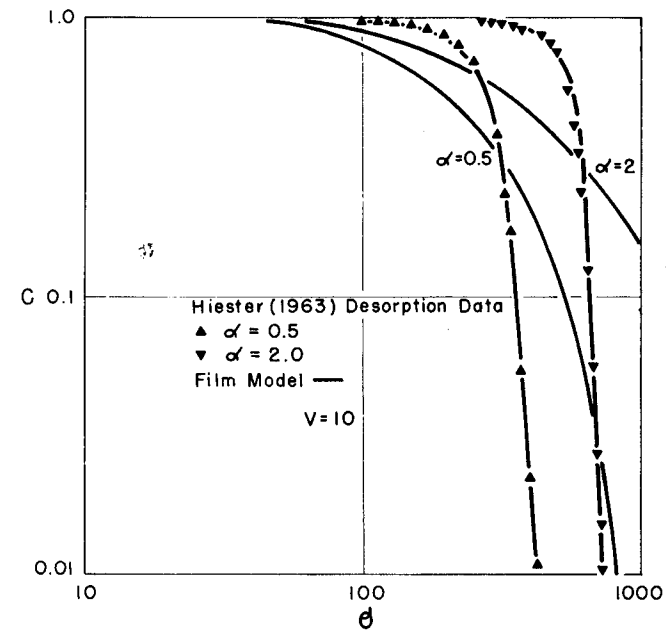

Fig. 11b. Comparison between depletion curves predicted by film model and kinetic model, c_0 = constant = 0.05.

cally at a pinched point near zero loading due to the convex curvature of the isotherm.

It should be noted, however, that the inlet gas composition c_0 and its corresponding adsorbent loading w_∞ also appear in the time parameter u in Equation (3b). Since K and c_0 do not appear together, as they do in C^*, their variation would have distinctly different effects upon the breakthrough and depletion phenomena. When the ratio c_0/w_∞ is factored out from the time parameter, the rate Equation (2) acquires a proportional multiplier

$$\frac{\partial W}{\partial u'} = \frac{c_0}{w_\infty}\left[C - \frac{W}{\alpha(1-W)+1}\right] \qquad (9)$$

where $u' = u(w_\infty/c_0)$ from Equation (3b). The ratio c_0/w_∞ is the inverse of the slope of the line segment drawn along the isotherm between the origin and the equilibrium point (w_∞, c_0). Figure 10a shows that with increasing values of K (assuming W_m is constant) the ratio c_0/w_∞ decreases (slope increases) at a fixed value of c_0. On the other hand, the same ratio increases in value (slope decreases) as c_0 is increased with K held constant, Figure 10b. Hence, with both c_0 and K affecting C^* in the same way in the driving force portion of the rate Equation (9), the differentiating factor becomes the multiplier c_0/w_∞. As this ratio decreases with increasing K, the sorption rate decreases, but as it increases with increasing c_0 the rate also increases.

Therefore, it would be expected that as K is increased at a constant c_0, the depletion curves and the breakthrough curves will be broadened due to the lowered mass transfer rates, that is, the slopes of the time profiles will be decreased. On the other hand, with the increasing K the adsorbent capacity is increased (Figure 10a). This, coupled with the reduced desorption rates, delays the depletion point. Similarly, the breakthrough points are also delayed at higher K values. These effects are illustrated in Figure 11.

The variation of the inlet composition results in sharper breakthrough and depletion curves with increasing c_0 (Figure 12). In this case there is a reinforcing contribution to the increased rate; not only does the multiplier ratio in Equation (9) increase with increasing c_0, but also the driving force term increases since C^* decreases with higher values of c_0. This is in contrast to the already discussed variation of the equilibrium coefficient K, in which case these effects oppose each other, that is, the ratio c_0/w_∞ decreases with increasing K, but as K goes up, C^* decreases and consequently the driving force increases.

The breakthrough points and the depletion points de-

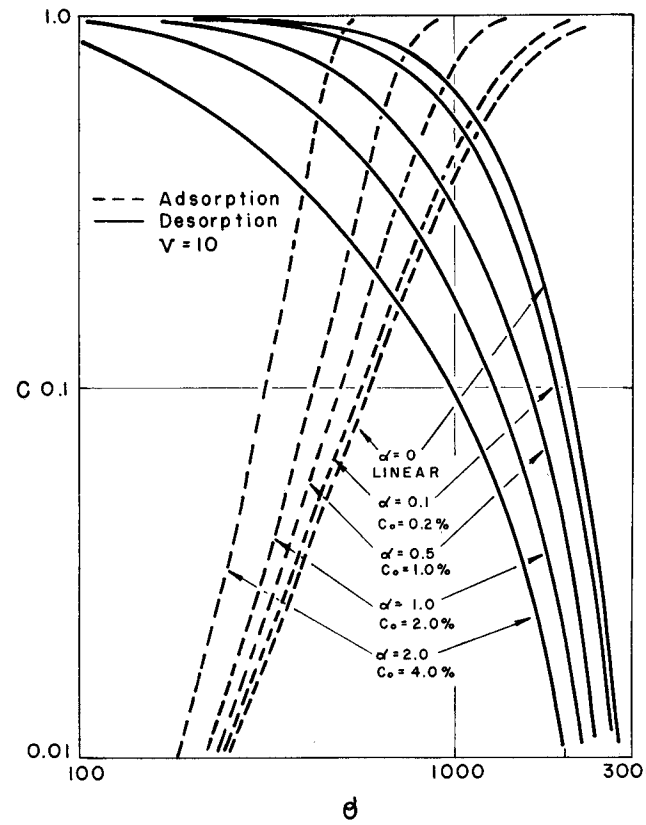

Fig. 12. Calculated breakthrough and depletion curves at various inlet compositions; K = constant.

crease with increasing c_0 because with the convex-favorable type isotherm the incremental capacity increase (Δw_e) is less than the corresponding supply rate to the column (Δc_0), Figure 10b. Thus, even though the mass transfer rates are increased, the column's capacity to retain the adsorbate is not increased proportionately; hence quicker breakthroughs will be observed. The results obtained by Antonson and Dranoff (1969) with an internal diffusion model confirm these trends with regard to the isotherm nonlinearity.

These predicted trends were demonstrated experimentally. Figure 13 shows the variation of depletion times with inlet composition for the three different gases (different K's) used in the current program (CO_2, C_2H_4, and C_2H_6).

Since the present model assumed that the velocity in the column was unchanged, and that the mass transfer coefficient which is usually velocity dependent was also constant, the only flow rate effects would be expected as it affects the residence times. Figure 14 shows the predicted and experimental volumetric throughputs as a function of the inlet gas velocity to the column.

DESIGN APPLICATIONS

Heretofore depletion curve data were not available in the literature, at least not for systems characterized by nonlinear isotherms. The present results are still restricted to somewhat limited systems, such as those which can be described by a film controlled mass transfer rate model. This is a rather severe restriction when porous adsorbents are being used, since in such cases internal transport within the particles is usually the controlling mechanism. Nor is this model particularly useful for cases where the heat of adsorption is relatively high, since under these conditions there are significant departures from isothermal behavior.

However, for systems where the stipulated model is a good approximation of the prevailing mechanisms, the data presented in this paper provide an easy method for design, with only the equilibrium coefficient K being determined experimentally. For example, if a stream with given feed composition c_0 and inert gas volumetric feed rate F is to be purified so that the effluent concentration of adsorbate is no higher than c_m, the following procedures may be followed to obtain the desired column dimensions and the appropriate operating conditions:

Adsorption

1. Select the adsorbent particle size distribution which will allow pressure drop limitations to be met, and calculate the constant A (w_∞ being available from equilibrium data).
2. From the given flow rate and particle dimensions establish the column diameter so that the desired turbulent flow regime prevails.
3. Using the properties of the gases and the specified pressure, temperature, and velocity data, calculate the mass transfer coefficient k_A from appropriate relationships (Vermeulen, 1958).
4. By arbitrarily setting a breakthrough time t_B, determine the time parameter u_A.
5. From the appropriate generalized plot $\alpha = Kc_0$, determine the distance parameter v_A by trial and error (first assume $T_{(1),A} = u_A$, find $v_{(1),A}$ which corresponds to $T_{(1),A}$ and $C_m = c_m/c_0$, then correct $T_{(2),A} = u_A - v_{(1),A}/A$, and find the improved $v_{(2),A}$, etc.).
6. Evaluate the height of the column from the proper value of v_A; $L = v_A V_A/k_A$.
7. Plot the concentration profile in the column by reading the values of C at the final T_A (established in step 5) corresponding to the distance parameters (v) within the column.

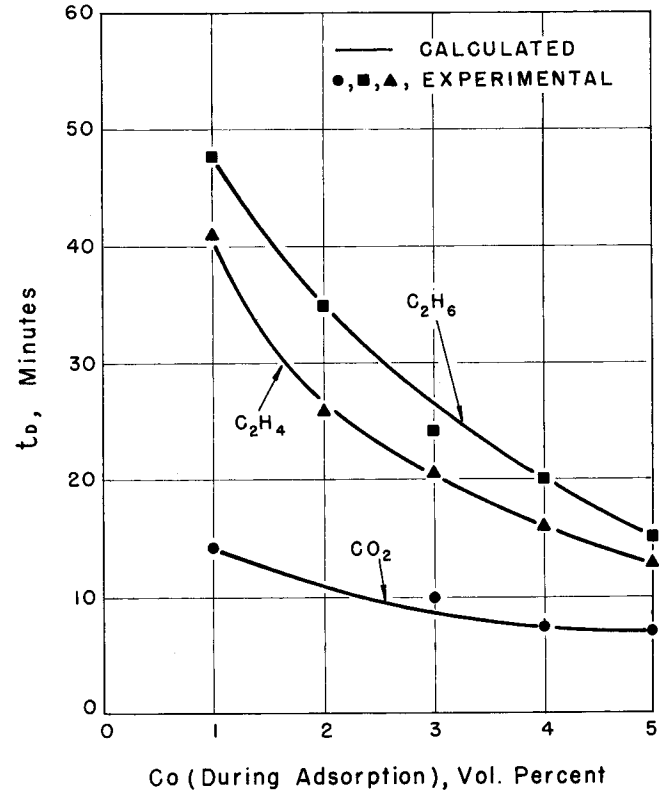

Fig. 13. Comparison of predicted and experimental depletion times; $C = 0.99$, $L = 180$ cm, $F = 10{,}000$ s.cm./min.

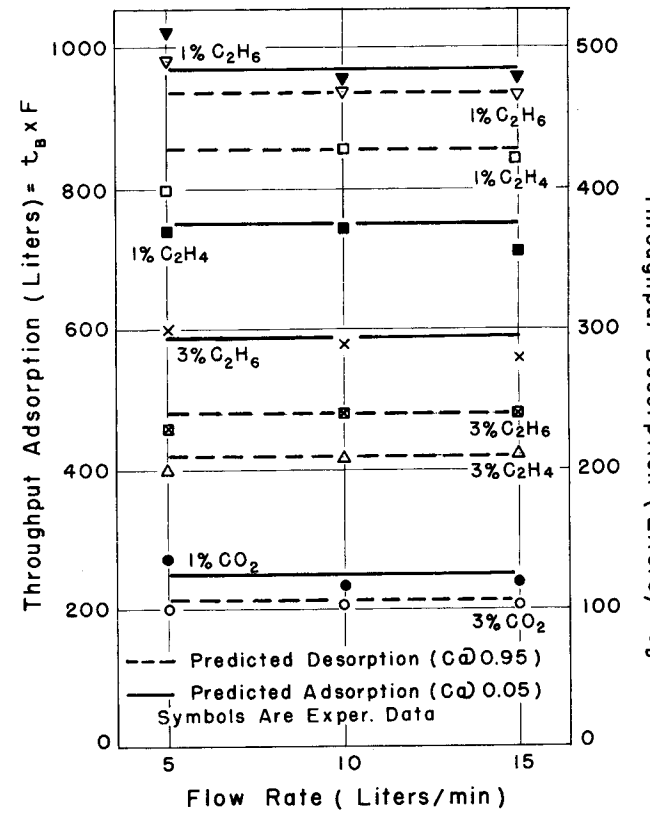

Fig. 14. Effect of gas flow rate on breakthrough times ($C = 0.01$) and depletion times ($C = 0.99$).

Desorption

8. Establish an equivalent column length for desorption; this is obtained from the profile prepared in the previous step, most conveniently the v_D which corresponds to $C = 0.5$. (This procedure compensates for the fact that the generalized depletion curves were calculated from an uniformly loaded bed.)

9. Corresponding to this equivalent v_D, find the appropriate value of the time parameter T_D that will give a suitably low effluent concentration in the desorbate (say $C_D = 0.005$).

10. Calculate $u_D = T_D + v_D/A$, using the value of A determined above.

11. Next calculate an apparent mass transfer coefficient for desorption $k_D = u_D \rho_B w_* / c_0 t_D$ with the time for desorption being set by operating policy criteria. For example, if a two-column system is to be used, $t_D = t_B$, or if a three-column option is preferred, $t_D = 2t_B$, etc.

12. Finally calculate the necessary gas velocity during the desorption step: $V_D = k_D L / v_D$.

Optimization of the process can be accomplished by assigning appropriate values to each of the design parameters and operating conditions, then repeating the calculations until a minimum cost is found. Of course, alternate design schemes may be developed; for example, one could just as readily calculate the effectiveness of an already built adsorption column system.

ACKNOWLEDGMENT

The authors wish to acknowledge the support of the National Science Foundation. Also, they would like to express their gratitude to Mrs. S. S. Hubbard and Messrs. C. A. Keisling and R. S. Knapik for their assistance in the preparation of the manuscript.

NOTATION

A = dimensionless coefficient $= \rho_B w_* / c_0 f$
B = dimensionless coefficient $= AV/kL$
c = gas phase composition, moles/volume
c_0 = inlet gas phase composition, moles/volume (occasionally values are given as volume %)
C = normalized gas phase composition $= c/c_0$
C^* = normalized equilibrium gas phase composition, see Equation (4)
f = void fraction of bed, volume void/bed volume
F = volumetric flow rate, volume of gas at s.t.p./time
$F_j(v)$ = gas phase composition distribution at the start of run
$G_j(v)$ = solid phase loading distribution at the start of run
k = mass transfer coefficient, moles/time/bed volume/concentration
K = equilibrium coefficient, (moles/volume)$^{-1}$
L = bed length, for example, cm
r = equilibrium parameter used by Vermeulen (1958) and Hiester et al. (1963), $r = 1/(1 + \alpha)$
t = time, for example, minutes
T = modified dimensionless time parameter, $u - v/A$ [related to the variable Z used by Hiester et al. (1963), $Z = T/v$]
u = dimensionless time parameter $= kc_0 t / \rho_B w_*$
v = dimensionless distance parameter $= kx/V$ [related to N_R used by Hiester et al., (1963), and referred to as the column capacity parameter]
V = constant superficial gas velocity, distance/time
w = solid phase loading, moles/weight of solid
w_* = solid phase loading in equilibrium with inlet gas composition, moles/weight of solid, see Equation (4)
W = normalized solid phase loading $= w/w_*$
W_m = monolayer loading as per Langmuir theory, moles/wt. of solid
x = axial position, for example, cm

Greek Letters

α = equilibrium parameter $= Kc_0$
θ = modified time variable, $t - fx/V$
ρ_B = bulk density of bed, weight of solids/column volume

Subscripts

A = adsorption
D = desorption

LITERATURE CITED

Acrivos, Andreas, "Method of Characteristics Technique," *Ind. Eng. Chem.*, 48, 703 (1956).

Antonson, C. R., and J. S. Dranoff, "Non-linear Equilibrium And Particle Shape Effects In Intraparticle diffusion Controlled Adsorption," paper presented at the 64th National AIChE Meeting, New Orleans (1969).

Chi, C. W., and Hanju Lee, "Separation Of n-Tetradecane From i-Octace-n-Tetradecane Mixture By 5A Molecular Sieves," *ibid.*

Eteson, D. C., and I. Zwiebel, "Hybrid Computer Solution Of The Simple Fixed Bed Adsorption Model," *AIChE J.*, **15**, 124 (1969).

Fukunaga, Paul, et al., "Mixed-Gas Adsorption And Vacuum Desorption Of Carbon Dioxide On Molecular Sieve," *Ind. Eng. Chem. Process Design Develop.*, 7, 269 (1968).

Gariepy, R. L., and I. Zwiebel, "Adsorption Of Binary Mixtures In Fixed Beds" presented at the 68th National AIChE Meeting, Houston, Texas (1971).

Gariepy, R. L., "Dynamic Behavior Of Gas Mixtures in Fixed Bed Adsorption Columns" Doctoral thesis, Worcester Polytechnic Inst., Mass. (1972).

Hiester, N. K., and T. Vermeulen, "Saturation Performance Of Ion-exchange And Adsorption Columns," *Chem. Eng. Progr.*, 48, 505 (1952).

Hiester, N. K., et al., "Adsorption and Ion Exchange," Chemical Engineers' Handbook, R. H. Perry, C. H. Chilton, and S. D. Kirkpatrick, (eds.), 4th Ed., Sect. 16, McGraw-Hill, N. Y. (1963).

Kondis, E. F., and J. S. Dranoff, "Non-isothermal Sorption Of Ethane By 4A Molecular Sieves," paper presented at 68th National AIChE Meeting, Houston, Texas (1971).

Kurochkina, M. I., and P. G. Romankov, "Kinetics Of The Process Of Desorption From A Porous Adsorbent In A Suspended Bed," *Zhur. Prikland. Khim.*, **33**, 2657 (1960).

Lapidus, Leon, Digital Computation For Chemical Engineers, pp. 168-175, McGraw-Hill, New York (1962).

Nassonov, P. M., "Adsorption Isotherms And The Kinetics Of Gas Sorption And Desorption On Heterogeneous Surfaces," *Zhur. Fiz. Khim.*, **35**, 118 (1961).

Rosen, J. B., "Kinetics Of A Fixed Bed System For Solid Diffusion Into Spherical Particles," *Ind. Eng. Chem.*, **46**, 1590 (1954).

Thomas, H. C., "Heterogeneous Ion Exchange In A Flowing System," *J. Am. Chem. Soc.*, **66**, 1664 (1944).

Timofeev, D. P., "On The Rate Of Desorption," *Zhur. Fiz. Khim.*, **32**, 2483 (1958).

Vermeulen, T., in Advances In Chemical Engineering, T. B. Drew, (ed.), V. 2, pp. 147-208, Academic Press, N. Y. (1958).

Young, D. M., and A. C. Crowell, Physical Adsorption Of Gases, pp. 106-110, Butterworth, Wash., D.C. (1962).

Zwiebel, I., and J. J. Schnitzer, "Desorption From Fixed Bed Columns Containing Activated Carbon," paper presented at 10th Intern. Carbon Conf., Bethlehem, Pa. (1971).

Manuscript received February 22, 1972; revision received May 23, 1972; paper accepted June 7, 1972.